Fabrication and optimization of a new polyethersulfone membrane integrated with powder activated carbon for landfill leachate treatment

Salahaldin M.A. Abuabdou[a], Zeeshan Haider Jaffari[b], Mohammed J.K. Bashir[c,*],
Ng Choon Aun[c], Sumathi Sethupathi[c]

[a]Department of Engineering Science and Applied Arts, University College of Science and Technology, Khan Yunis, Gaza Strip, Palestinian Authority, email: sabdou6@gmail.com
[b]Department of Environmental Engineering and Management, Chaoyang University of Technology, No. 168, Jifeng E. Rd, Wufeng District, Taichung 413310, Taiwan, email: engr.zeeshanhaiderjaffari@gmail.com
[c]Department of Environmental Engineering, Faculty of Engineering and Green Technology (FEGT), Universiti Tunku Abdul Rahman, 31900 Kampar, Perak, Malaysia, Tel. 605-4688888 Ext: 4559; Fax: 605-4667449; emails: jkbashir@utar.edu.my (M.J.K. Bashir), Ngca@utar.edu.my (N. Choon Aun), sumathi@utar.edu.my (S. Sethupathi)

A B S T R A C T

A wide range of highly concentrated non-biodegradable organics have existed in stabilized landfill leachate, which is highly dangerous to the environment. Although various purification processes have been invented for leachate treatment, yet advanced membrane filtration is still one of the most environmentally friendly processes for stabilized leachate treatment. Herein, a new polymeric membrane was fabricated through the integration of powder activated carbon (PAC) on the surface of polyethersulfone (PES) using the phase inversion technique. The newly fabricated membrane was optimized using response surface methodology (RSM). The synthesized membrane was successfully applied as a cross-flow ring towards the filtration of stabilized leachate. The results proposed that the filtration efficiency of the membrane was highly boosted after the incorporation of PAC. The optimal removal efficiencies of the proposed membrane (1.0 wt.% PAC, 14.9 wt.% PES) was 22%, 48.71% and 35.34% for NH_3–N, colour and chemical oxygen demand, respectively. Transmembrane pressure and water flux values were 0.67 bar and 61 L m^{-2}, respectively, using optimized conditions, which were again improved after the PAC incorporation. Besides, the membrane performances in terms of contaminant elimination, water permeation and numerous morphological characterizations were systematically investigated. Regardless of the partial accomplishments, which could further be enhanced through the utilization of hydrophilic additives, the current report offers a novel roadmap to fabricate PES- PAC membranes and their optimization using the RSM tool.

Keywords: Filtration treatment; Membrane fabrication; Performance optimization; Stabilized landfill leachate

1. Introduction

Sanitary landfills are the widely applied technique to tackle municipal solid waste (MSW). Inappropriately, the majority of these landfills did not fulfill the normal discharged limits [1]. In developing countries like Malaysia more than 80% of the MSW produced was received by open duping and landfill sites [2]. It resulted in the generation of highly contaminated leachate, which is the liquid generated due to the precipitation above these solid litters and could be toxic to the surrounding environment. This leachate could contaminate the sources of fresh water if not carefully treated before discharging to the environment [3]. Stabilized leachate, which is more than 10 years old, has

* Corresponding author.

lower 5-day biochemical oxygen demand (BOD_5)/chemical oxygen demand (COD) ratio. Thus, it is almost impossible to treat this kind of leachate using some biological treatment technique [4]. Until now, various purification techniques such as adsorption [5], coagulation [6], advanced oxidation [7], electro-Fenton [8], and combinations of these processes [9,10] have been successfully introduced to eliminate the organic contaminates from stabilized leachate. Among these techniques, membrane filtration could be one of the most suitable purification process [11]. The membranes acted as a selective barrier to achieve the objective of separation and purification. Nonetheless, there are still some shortcomings in membrane technology like membrane fouling upon the higher contaminant concentration [12]. Fouling could affect the separation efficiency as well as permeability of membrane, which are the vital factors in the membrane filtration [13]. Several strategies including pre-treatment of feed [14], optimization of operating parameters [15], selection and modification of membrane [16], hydraulic flushing [17] and applied field enhancement [18] have been performed to alleviate membrane fouling and water flux rate. Under different circumstances, the workability of membrane can be improved through the membrane characteristics and performance of treatment process. Hence, investigation on membrane characterization can be separated into four groups: membrane activity (permeability, surface wettability, average pore size and porosity); morphological characterization (surface chemistry and roughness, and external and internal membrane texture); treatment efficiency (separation performance); and antifouling evaluation (pore size decreasing and cake formation) [19].

Synthetic polymers such as polypropylene (PP), polyvinylidene fluoride (PVDF), polysulfone (PS) and polyethersulfone (PES) are commonly applied in the membrane fabrication due to their higher flux, antifouling ability and separation efficiency [20]. Among all these synthetic polymers, PES polymer are proved to be an ideal membrane fabrication material due its durability [21], good thermal stability and higher chemical resistance [22]. Besides, the PES polymer can also help to extend the membrane life as well as reduce the damage caused by the concentrated pollutants [23]. However, the PES membranes antifouling capability could be enhanced due to its hydrophobic nature [24]. Many researchers have successfully applied dry-wet phase inversion technique to boost their membrane performance [25]. For instance, Zhou et al. [26] developed an ultrafiltration PES membrane using nanoparticles of titanium dioxide (TiO_2) and polyvinylpyrrolidone (PVP) as blended additives to increase the fouling resistance and water permeability. Addition of PVP-TiO_2 increase the average pore size and porosity of membrane, leading to the higher flux and hydrophilicity of membrane with more than 91.4% removal performance against sulfonamide antibiotics water. Moreover, polyethylene glycol and poly(acrylic acid) were also applied in the fabrication of membrane through chemical reaction with a key focus of enhancing hydrophilicity. Their batch filtration experiments clearly exhibit an increase in critical flux and a declined fouling rate. Similarly, various reports presented effective ways to boost the antifouling abilities of PVA-based membranes due to their hydrophilic properties [27,28].

Recently, the incorporation of activated carbon (AC) on the surface of membrane has proved to be an effective way to boost the membrane rejection performance [29]. The utilization of AC in membrane is a relatively new technology for the elimination of organic contaminates for wastewater, which not only enhance the adsorption capacity of AC but also improve the particle removal capabilities of membrane [30].

To date, there are quite a number of studies which had clearly provide that the usage of powder activated carbon (PAC) can significantly improve the filterability of membranes [13]. However, evaluation of PAC addition into PES flat sheet membranes with different concentrations in terms of their treatment efficiency and productivity has not been carried out so far. Therefore, the current study was performed to observe the potential of incorporating PAC; for the first time, into the PES polymeric membrane for stabilized landfill leachate purification. Furthermore, fabricated membrane was optimized using response surface methodology (RSM) technique and the membrane properties and morphologies were systematically characterized.

2. Materials and methods

2.1. Collection of leachate

Leachate sample was taken form Sahom landfill site (4° 23′ 25″ N, 101° 10′ 57″ E), located in Perak, Malaysia, which is an operative landfill site with a daily production of 100 tonnes of MSW in average [31]. After collection of leachate sample, it was stored in a refrigerator at 4°C. Initial leachate characterization was performed using standardized methods of water and wastewater [32]. All measurements including dissolved oxygen (DO), colour, COD, BOD_5 and ammoniacal nitrogen (NH_3–N) were undertaken in triplicates. All chemical analysis was performed according to the Standard Method of Water and Wastewater by APHA (2012).

2.2. Fabrication materials

The PES polymer (Kynar® 740) with a molecular weight of (232.26 g mol⁻¹) was purchased from Afza Maju Trading (Terengganu, Malaysia), and utilized after drying for 24 h at 70°C. 1-Methyl-2-pyrrolidinone (NMP, 99.5%) was obtained from Sigma-Aldrich. Methanol, (99.8%) was supplied by Chem Soln. Ultrapure distilled water (DI) was utilized throughout the experiments. PAC was purchased from R&M Chemicals. The AC was in charcoal based and consists of sulfide, chloride, calcium, sulphate, iron, lead, zinc and copper. This PAC density was 1.8–2.1 kg m⁻³ with ranged values of particle size (0.02–50 μm) and pH (4–7). Particle size analysis (PSA) and field-emission scanning electron microscopy (FESEM) tests were used to investigate the distribution and the size of PAC particles, respectively. All of these chemicals was of analytical grade and applied without additional treatment.

2.3. Experiments design and optimization process

Central composite design (CCD) is the design method applied in RSM for the membrane fabrication's experimental design [33]. Both CCD and RSM were run by version 8

from the Design-Expert. For membrane dope solution design, two factors which are the polymer (PES) weightage and the additive (PAC) weightage were set into the CCD. Based on preliminary experiments and literature reports [34,35], the total mass of the fabricated membrane dope was fixed at 100 g, which represents 100% of the dope weight. Thus, every 1 g dope element was equal to the 1% weightage. The dosage of the PES was adjusted ranging from 10 to 18 g and the PAC dosage was fixed between 0–2 g. On CCD, Alpha value was selected to be 1.0 and thus the center points were 14.0 and 1.0 wt.% for the polymer content and additive content, respectively. The rest of the dope weight (to complete 100 g) is the NMP solvent. The entire PES/PAC concentration was reserved at 20% (as maximum) and 10% (as minimum), as more than 20% concentration caused extremely high viscosity, and was difficult to be casted on the glass, while clumsy non-thick membrane was resulted using concentration less than 10%. Five responses including COD efficiencies, colour and NH_3–N, maximum trans-membrane pressure (Max. TMP) and pure water flux were also set into the CCD to have the full design of experiments. The influence of various parameters was optimized by RSM using a combination of statistical and numerical techniques. In the current work, nine experiments were reinforced with four replications to assess the pure error [36]. The 13 different membranes were applied in double repetition and have their effluent collected. Quadratic model for every response was investigated by variances analysis (ANOVA) to identify the results significancy, and to find the represented quadratic model after eliminating irrelevant terms. The frontal sign of each model term signifies to either antagonistic or synergistic effect on the response when it is positive or negative, respectively [4]. In RSM, it does mention that Prob. > F less than 0.050 specifies model terms are significant and Prob. > F with the values greater than 0.10 indicates model term is not significant. Whereas "not significant" in the description of lack of fit is regarded a decent model, as it means the experimental reading is fitting the model [37]. Additionally, a good experimentally fitted data will have a higher coefficient (R^2) value. The higher the R^2 values, the closer the experimental data towards the predicted graph model by the RSM [38,39]. Selection of the best membrane takes into consideration the membrane purification performance. Desirability value closer to 1.0 used to be selected as the ideal design for the data.

2.4. PES-PAC membrane fabrication

2.4.1. Dope preparation

To produce the polymeric membrane, PES and NMP were applied as polymer and solvent, respectively. Fig. 1 illustrates the process used for the dope preparation. Initially, the polymeric PES was entirely dissolved in the NMP solvent at a temperature ranged between 60°C–70°C using a heating mantle (Fig. 1a). In order to achieve a better permeate flux of the synthesized membrane the heating mantle temperature should always maintained within the above stated range [21]. The dope solution containing dissolved PES polymer in the NMP solvent was then infused into a clean Schott bottle. After that, the required amount of PAC was inserted into the dope solution to generate the dope for hybrid membrane. Lastly, the Schott bottle contained the dope solution was placed into a ultrasonicated bath for 8 h for confirming the homogeneous mixing of the additives without any air bubbles raised in the prepared dope [40].

2.4.2. Membrane casting

A membrane casting machine (semi-automated) was applied to synthesize a flat sheet membrane using the dry-wet phase process, as shown in Fig. 2a. The membrane was produced at temperature 27°C–30°C with an approximate thickness around 60 μm based on literature reports [41,42]. After 60 s of membrane casting above the glass board, it was submerged into a distilled water (DW) basin for 180 s (Fig. 2b). As a result, a thin layered polymeric film was generated, which part itself away from the glass plate. Later, the newly produced membrane was transferred into a DW coagulation bath and remained for 24 h. Afterwards, methanol bath was used for 8 h as shown in Fig. 2c, to perform a post-treatment to ensure the excess solvent in the membrane can be removed out completely [43]. Finally, drying of the membrane was done for 24 h at the ambient temperature with 60% humidity, as shown in Fig. 2d, to be ready to use in the filtration process [13].
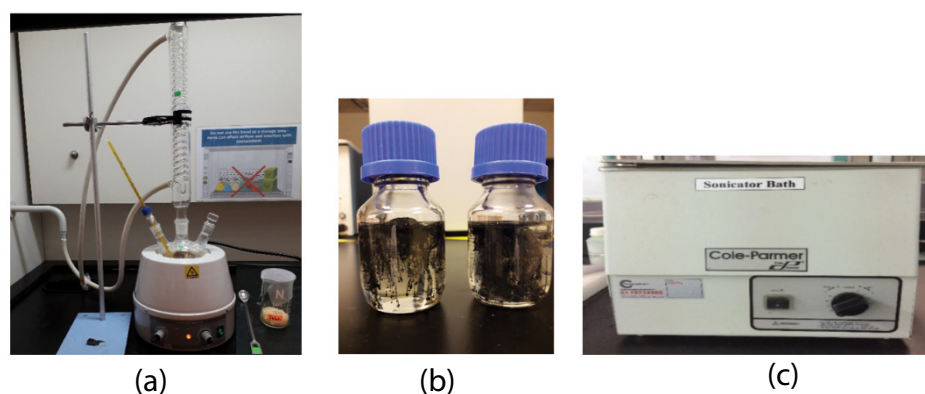

(a)   (b)   (c)

Fig. 1. PES-PAC membrane dope preparation steps. (a) Polymer dope preparation, (b) adding of PAC and (c) membrane dope sonicator.
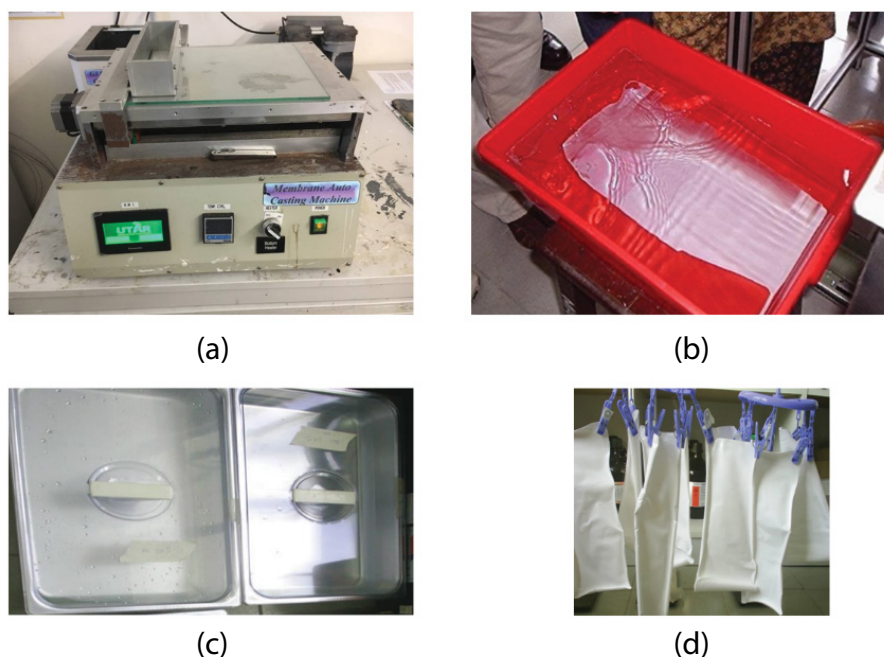
(a)

(b)

(c)

(d)

Fig. 2. The PES-PAC membrane casting process. (a) Flat sheet membrane casting, (b) membrane solidification, (c) membrane neutralization and (d) membrane drying.

2.5. Membrane performance and characterization

The produced membranes have been characterized to investigate their treatment efficiencies, fouling and permeability properties and surface morphologies. To ensure the accuracy of the findings, all of the tests have been duplicated. Each time a fresh membrane has been utilized to investigate their characteristics and performance.

2.5.1. Treatment efficiency

The membrane filtration performance was investigated using laboratory scale cross-flow filtration setup with a 3.34 cm disc diameter, as exhibited in Fig. 3. The membrane rejection capabilities were studied against the treatment of landfill leachate. Before each experiment, initial characterization of leachate was measured to eliminate the small errors occurred due to the minor changes in organics concentration with time. The steady flux for all individual membranes was acquired by a constant (200 mL min⁻¹) flow for 120 min. The volume of permeate along with the recorded transmembrane pressure were noted down under the flow of 200 mL min⁻¹ for various intervals of time.

Final leachate characterizations were evaluated in terms of removing efficiencies for the COD, colour and NH_3–N pollutants via Eq. (1):

$$\text{Removal efficiency \%} = \frac{\left(C_F - C_P\right)}{\left(C_F\right)} \times 100\left(\%\right) \tag{1}$$

where C_F is the contaminant concentration at the feed (mg L⁻¹) and C_P is the contaminants concentrations in the permeated solution (mg L⁻¹). All contaminants concentrations

Fig. 3. CFR test configuration (filtration set).

were checked using the UV-V spectrophotometer (Hach DR6000) in prior and post of filtration practice.

2.5.2. Productivity of membrane

Pure flux plays a dynamic role in the membrane productivity evaluation. Permeability of membrane was investigated through the pure water flux, which measured via a dead-end filtration apparatus, as illustrated in Fig. 4. A metallic ring having 5 mm average pore size and 8.76 cm² effective permeate area was applied to support the membrane. Initially, the impurities present in the membrane was removed by submerging the membrane in DW for 30 min.

Fig. 4. Dead-end test (pure water permeation set-up).

Then, a stable flux was achieved by pre-compacting the membrane with N_2 gas at a pressure of 30 KPa for 2 min. After 30 min, the permeated water volume was noted at a similar pressure of 30 KPa. The pure water flux can be calculated using Eq. (2):

$$J = \frac{V}{A \times t} \left(L / m^2 \cdot h \right) \tag{2}$$

where V is the permeated pure water volume (L), A is the membrane effective surface area (m^2), and t is the time of permeation (h).

2.5.3. Antifouling valuation

Throughout the membrane filtration process, the overall decrease in flux alongside the improvement of transmembrane pressure were mainly caused by either membrane fouling or concentration polarization or a combination of both [44]. Both of these components can be attained from the experimental data using both of the leachate permeate flux and maximum transmembrane pressure (Max. TMP) values that is measured by the cross-flow ring test. Max. TMP was applied to indicate the antifouling ability of fabricated membranes [45].

2.5.4. Morphological characteristics

It is a well-known fact that the membrane properties and performance are highly depended on its morphology (pore size, surface texture and microstructure). Therefore, investigation of membrane morphologies considered as a significant factor in the effectiveness evaluation of the produced membranes.

The Fourier-transform infrared (FTIR) spectrum of the fabricated membranes were recorded using a Perkin Elmer Lambda 35 in the range of 400–4,000 cm^{-1}.

FESEM was applied to record the surface and cross-sectional morphologies of the fabricated membrane using Quanta FEG 450. The cross-sectional morphologies were investigated by fracturing the membranes in liquid nitrogen and immediately cutting them after air drying. FESEM measurement start by placing the sample on carbon tape, which was attached with the sample stub. The sample was also coated with the platinum nanoparticles in auto fine coater (JFC-1600) before performing the analysis.

An atomic force microscopy (AFM) was also applied to study the surface morphologies and roughness of the synthesized membranes using Dimension 5000 (Bruker AXS). Herein, membranes were cut into small square pieces (1 cm × 1 cm) and pasted on a glass slide. Sample scanning were performed using a probe-optical microscope on tapping mode and images of 10 μm × 10 μm were taken by AFM. The root-mean-square roughness (R_q) and average roughness (R_a) was applied to measure the surface roughness for each membrane.

Porosity of membrane could be easily defined as the pore's volume divided by the membrane total volume. Wet membranes were weighed after carefully wiping the surface (W_w). Afterwards, these membranes were dried in an oven at 50°C for 24 h and weighed again (W_d). The porosity of membrane ε (%), was measured by gravimetric method using Eq. (3) [25].

$$\varepsilon = \frac{\left(W_w - W_d \right) / \rho_w}{\dfrac{W_w - W_d}{\rho_w} + W_d / \rho_p} \times 100\% \tag{3}$$

where W_w is the weight of wet membrane (kg), W_d represents the weight of dry membrane (kg), ρ_w was the density of water (1,000 kg m^{-3}), ρ_p, the polymer density (1,770 kg m^{-3} for PES).

Based on the measured distilled water flux, the average pore size (d) of the membrane was calculated by the Guerout–Elford–Ferry equation [46].

$$d = \sqrt{\frac{(2.9 - 1.75\varepsilon) \times 8\delta l V}{\varepsilon \times A \times \Delta P \times t}} \, (m) \tag{4}$$

where ε is membrane porosity (%), δ, the water viscosity (8.9 × 10^{-4} Pa·s), l represents membrane thickness (60 × 10^{-6} m), V is the volume of the distilled water penetrating through the membrane (m^3), t was the experimental time interval (s), A the effective membrane surface area (m^2), and ΔP was the working pressure (30 kPa).

3. Results and discussion

3.1. Landfill leachate characteristics

Table 1 displays the key characteristics of the raw leachate sample of more than a decade old. The lower BOD$_5$ to COD ratio (0.074) was another strong indication of highly stabilized leachate sample [3]. The other quality parameters of leachate such as COD, BOD$_5$, NH$_3$–N, colour and pH values were around 1,188 mg L^{-1}, 89 mg L^{-1}, 313 mg L^{-1}, 1,360 PtCo L^{-1} and 8.33, respectively. These obtained values were also compared with the standard discharged limits set by the Malaysian Environmental Quality was conducted (Table 1) [47]. As shown in Table 1, the COD,

colour and NH_3–N concentration found to be extremely greater than the standard discharged limits.

3.2. PAC characterization

Analysis test of the particle size was conducted to investigate the particle size distribution of fine samples in terms of volume. The particle size distribution of PAC sample is shown in Fig. 5a. It can be seen from Fig. 5 that PAC has small particles size which varied between (0.02–50 μm) in diameter. The average particle diameter of the PAC is 25 μm. It is evident from Fig. 5a that the distribution curve of PAC particles could be counted a uniform-distribution curve. The percentage of adsorption is higher for those adsorbents have smaller particle size because of the availability of more surface area [48]. The surface morphology of PAC was visualized via FESEM, with a magnification of 10,000× as shown in Fig. 5b. FESEM micrographs of PAC, shows uniform size particles which confirmed the results obtained from the particle size analysis. To some extent, the PAC surface having small cavities, pores and more rough surfaces indicating the presence of interconnected porous network. Increasing the particles' number of an adsorbent material by decreasing its particles size resulted in increasing the adsorption surface area and thus the material adsorption characteristics [49].

3.3. Membrane filtration findings

Herein, a relationship among the independent factors (PVFD and PAC dosage in membrane) and responses (COD, NH_3–N, colour removal, Max. TMP and pure water flux) was thoroughly investigated. There were 13 different experiments performed on the PES and PAC composition based on the central RSM composite design, as shown in Table 2. Cross-flow ring (CFR) test was performed to investigate the pollutants removal efficiency together with the Max. TMP, while dead-end test was executed to measure the pure water flux.

The COD, colour and NH_3–N removal efficiencies were found to be around 14.8–37.2, 14.6–56.3 and 7.5–23.8%, respectively, while the pure flux and Max. TMP were ranged between 26.2–127.7 L m^{-2} h^{-1} and 0.42–1.00 bar, respectively. ANOVA analysis was performed for the further investigation on the obtained experimental results.

Table 2 depicts an improvement in the contaminant's removal efficiency of membrane to some extent upon the

Table 1
Raw leachate characteristics

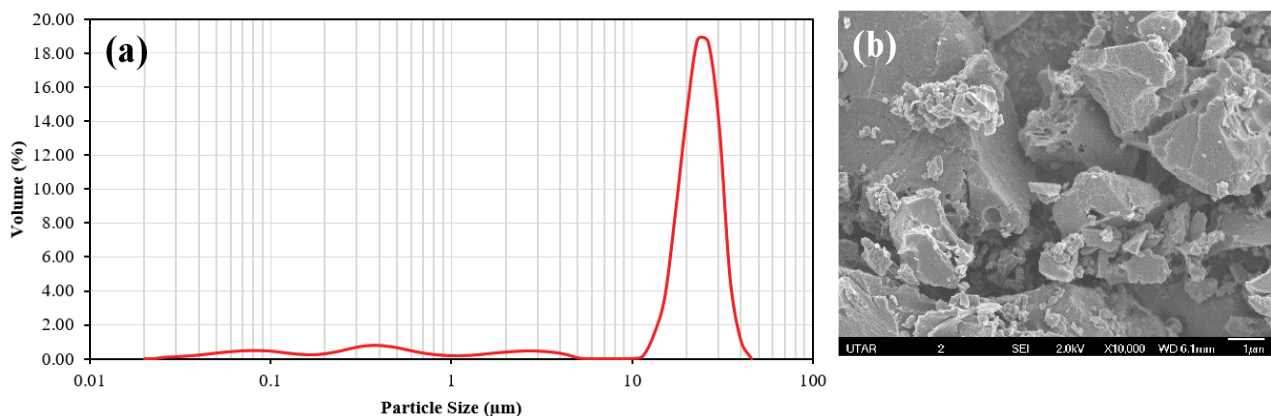| Parameter	Unit	Value range	Average	Malaysia Discharge Standards
DO	mg L^{-1}	2.43–5.19	3.81	–
COD	mg L^{-1}	846–1,530	1,188	400
BOD$_5$	mg L^{-1}	55–122	89	20
BOD$_5$/COD	–	0.065–0.080	0.074	0.05
Colour	PtCo L^{-1}	1,040–1,680	1,360	100
NH$_3$–N	mg L^{-1}	164–462	313	5
Suspended solids	mg L^{-1}	75.0–80.0	77.5	50
pH	–	7.97–8.68	8.33	6.0–9.0
Turbidity	NTU	15.9–70.2	43.1	–
Electrical conductivity	mS	13.22–22.77	18.00	–
Temperature	°C	27–30	28	40

Fig. 5. (a) Particle size distribution of PAC and (b) FESEM image of PAC.

increase in both PES and PAC concentration. When PAC and PES concentration is higher than 1.0 and 14 wt.%, respectively, the removal efficiency starts to be decreased. This behavior was credited to the combination of impacts among the additive and polymer in dope. This leads to creating large volume voids with increasing polymer dosage and permit a passage to the smaller particles from the membrane [50].

3.4. Removal efficiency of contaminants

Table 3 depicts the empirical model using the data obtained from COD, colour and NH_3–N removals. F-values of the model together with the low probability values ($P > F > 0.05$) clearly suggested that the models were significant for all responses.

The lack of fit F-statistic was statistically not significant, as the values of (P) were higher than 0.05. A significant lack

Table 2
Experimental results for the PES-PAC membranes (RSM design)

Run order	Factors		Responses				
	PES (wt.%)	PAC (wt.%)	Removal efficiency (%)[a]			Pure water flux[b] (L m^{-2} h^{-1})	Max. TMP (bar)
			COD	Colour	NH_3–N		
1	10.00	0.00	14.8	15.1	10.9	90.2	0.46
2	10.00	2.00	29.1	42.3	7.5	127.7	0.42
3	12.00	1.00	32.2	44.6	18.3	89.3	0.48
4	14.00	0.50	28.2	39.6	19.6	64.0	0.66
5	14.00	1.00	37.2	56.3	23.8	79.9	0.67
6	14.00	1.00	35.5	50.3	19.3	72.9	0.63
7	14.00	1.00	35.5	56.2	21.3	72.2	0.62
8	14.00	1.00	35.7	51.1	21.5	70.3	0.61
9	14.00	1.00	32.2	51.5	19.9	69.9	0.60
10	14.00	1.50	33.2	52.7	19.2	83.1	0.55
11	16.00	1.00	37.1	41.0	22.5	31.8	0.68
12	18.00	0.00	29.1	26.7	21.2	26.2	1.00
13	18.00	2.00	20.9	15.6	17.3	32.9	0.78

[a]Estimated by Eq. (1);
[b]Estimated by Eq. (2).

Table 3
ANOVA results and quadratic models of PES-PAC membranes for COD, colour and NH_3–N elimination

Source	COD removal (%)		Colour removal (%)		NH_3–N removal (%)	
	F-value	Prob. > F	F-value	Prob. > F	F-value	Prob. > F
Model	25.62	0.0002 (S)[a]	31.93	<0.0001 (S)[a]	24.34	0.0003 (S)[a]
A-PES (wt.%)	4.34	0.0759	3.89	0.0840	55.81	0.0001
B-PAC (wt.%)	4.19	0.0800	5.69	0.0441	6.37	0.0396
AB	32.25	0.0008	21.10	0.0018	0.032	0.8634
A^2	0.42	0.5375	97.03	<0.0001	0.24	0.6372
B^2	12.18	0.0101	–	–	3.62	0.0988
Lack of Fit	1.39	0.3665 (NS)[b]	3.27	0.1386 (NS)[b]	0.17	0.9088 (NS)[b]
	Std. Dev.	1.98	Std. Dev.	4.28	Std. Dev.	1.40
	Mean	30.85	Mean	41.69	Mean	18.64
	R^2	0.9482	R^2	0.9411	R^2	0.9456
	Adj. R^2	0.9112	Adj. R^2	0.9116	Adj. R^2	0.9067
	C.V. %	6.42	C.V. %	10.26	C.V. %	7.52
Model equation coded, (wt.%)	+34.80 + 1.94A + 1.91B – 5.63AB + 2.60A^2 – 14.00B^2		+50.80 – 3.98A + 4.81B – 9.82AB – 26.30A^2		+20.99 + 4.93A – 1.67B – 0.12AB – 1.40A^2 – 5.40B^2	

[a]Significant;
[b]Not significant.

of fit suggests that there may be some systematic variation unaccounted for the proposed models. The correlation coefficient value (R^2) resulted in the present study were (0.9482) for COD removal, (0.9411) for colour removal and (0.9456) for NH_3–N removal. Zielińska et al. [10] stated that the correlation coefficient should minimum be around 0.80 for a good fit of a model.

In the current study, all insignificant model terms which have limited effects were eliminated from the study to improve the model. Based on the findings, the response surface models for COD, colour and NH_3–N removal efficiency was constructed to predicting responses, which were considered reasonable. The final regression models in term of their coded factors are expressed by the second-order polynomial equations and are presented in Table 3.

Typically, it is vital to study the effect of the operational factors on the different responses. The effect of PES and PAC concentration on the responses of NH_3–N, colour and COD removals over PES-PAC membranes could be evaluated using perturbation and 3D response surface plots (Fig. 6). Perturbation plots show the comparative effects of independent variables on the responses. For instance, in Fig. 6, the different sharp curvatures in PES concentration (*A*) and PAC concentration (*B*) show that the three responses (NH_3–N, colour and COD removal efficiency) were very sensitive to the fabrication variables but with different behaviors. In other words, PES and PAC contents have main function in the treatment process under the experimental conditions.

Despite that incorporating of PAC into membrane has enhanced the NH_3–N, colour and COD removal, the filtered leachate is still did not met the Malaysian standard discharge limits (Table 1). This is because of the highly concentrated pollutants of leachate that resulted in reducing of membrane efficiency owing to the clogging caused by influent SS component. So a pre-treatment process like PAC adsorption is suggested to be used before using the membrane treatment [33].

3.5. Pure flux and transmembrane pressure studies

The pure water flux is directly indicating the membrane permeability, however, membrane fouling incident can be evaluated by the TMP measurement, where the increasing of TMP could indicate a membrane fouling potential. By applying the factorial regression analysis on the experimental data related to PES-PAC membranes, both of Max. TMP and pure water flux responses were well agreed to a linear model of the second degree as shown in the ANOVA analysis presented in Table 4. The final linear models obtained for each response has been expressed by the first order polynomial equation as presented in the last raw of Table 4.

The pure water flux fitted model suggests a large *F*-value (53.56), suggests that the model is significant. As the value of "Prob. > *F*" of all terms are less than 0.050 suggest that all the model terms are significant. Based on their *F*-values, the PES concentration term (*A*) has the highest influence on the model, followed by PAC concentration term and lastly the combination term. The term of PAC concentration presents a positive impact on flux, hence, the pure water flux was raised only with enhancing PAC contents in

the membrane. While in contrast, it is decreased with the increasing of the PES content of a membrane.

On the other hand, the suggested model of Max. TMP was significant with a high *F*-value (49.62), as can be seen from Table 4. Based on its effect on the model from the highest to the lowest, the model terms can be arranged as follows: PES content, PAC content and the combination between both of them, with *F*-values of 131.07, 13.01 and 4.78, respectively.

Besides, both of the models display a non-significant lack of fit *F*-value, which indicates that well fitted models have been selected to present the experimental results with minor pure errors [15].

The R^2 values obtained in the present study for both pure flux and Max. TMP were 0.9470 and 0.9430 respectively. The high value of R^2 represents good agreement between the observed and the calculated results within the experimental ranges [37].

Based on these findings, the obtained response surface models in the current work for predicting the two responses (Max. TMP and pure flux) were considered reasonable.

The influence of integrated PAC and the interaction of content's concentrations on the Max. TMP can be explored by the 3D response surface and perturbation plots, as shown in Fig. 7. From perturbation plots at Fig. 7, it is easy to notice that pure flux and Max. TMP responses are very sensitive to the experimental factors and to conclude that both of them has a different (inversed) behavior regarding the PES and PAC concentration values.

The perturbation plots depict that the increasing of PES concentration led to a sharp reduction in the pure flux where the best value of pure flux existing at 10.0 wt.% PES. On the other hand, when PES content was improved on the fabricated membrane, the Max. TMP increased rapidly, and its highest value found using 18 wt.% PES. These findings concluded that lower concentration of PES helped in best properties for both membrane permeation and antifouling ability, as well.

3.6. Fabricated membrane characterization

The morphology of produced membrane can explain the effect of dope composition on membrane performance. A collection of membranes composed from different concentrations of PES and PAC (wt.%) were chosen from the fabricated membranes to represent the different membrane compositions, and consequently to be investigated by the morphological studies. These membranes were: FM1 with the content of (10.0 wt.% PES-0.0 wt.% PAC) to represent minimum PES concentration with no PAC; (10.0 wt.% PES-2.0 wt.% PAC) to represent minimum PES with high PAC which denoted as FM2; (14.0 wt.% PES-1.0 wt.% PAC) to represent intermediate composition of both PES and PAC and named as FM3; and finally FM4 with 18.0 wt.% PES and 0.0 wt.% PAC to represent maximum concentration of PES without PAC.

The FTIR spectrum of PES-PAC fabricated membranes with the various compositions is illustrated in Fig. 8. It is clearly observed from Fig. 8 that membranes displayed semi-typical distinctive spectra along the range of 4,000 and 400 cm^{-1}. Characteristic chemical groups were witnessed in

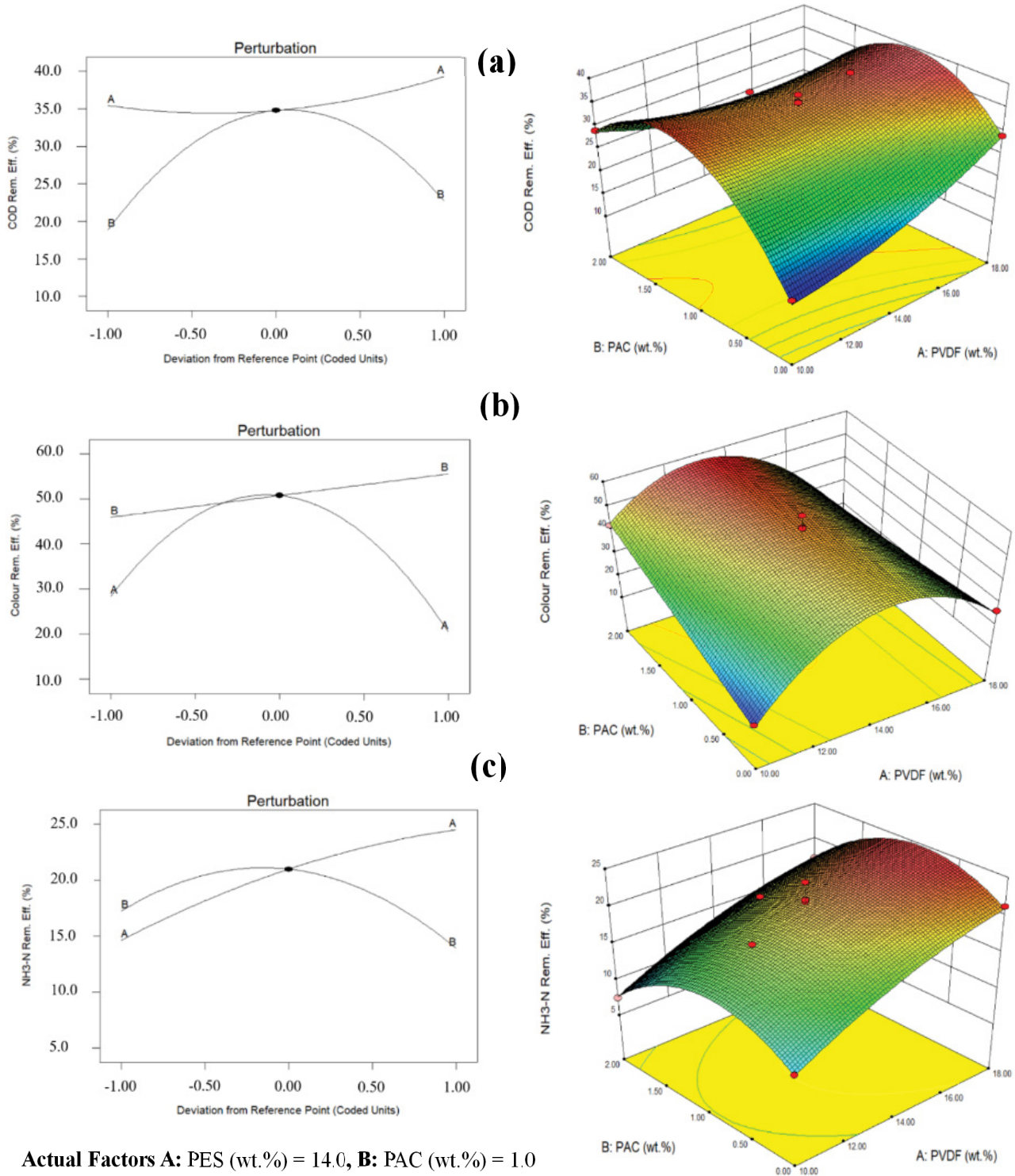**Actual Factors A:** PES (wt.%) = 14.0, **B:** PAC (wt.%) = 1.0

Fig. 6. 3D response surface (right) and perturbation plots (left) of PES-PAC synthesized membrane for the filtration performances of (a) COD, (b) colour and (c) NH$_3$–N.

all of the membrane samples at wavenumber 490; 590; 875; 1,070; 1,400; 2,370; 2,990 and 3,020 cm^{-1} with altered vibrations strength depends on the different membrane compositions. The spectrum shows bands at 2,990 and 3,020 cm^{-1}, which credited to the symmetric and asymmetric C–H

stretching vibrations appeared from the applied ketones and carboxylic acids [51], while the bends around 1,070 and 1,400 cm^{-1} presented the C–F related peaks deformation in PES. It is easy to notice that the fabricated membrane with higher PES content got higher peak values compared with

Table 4
ANOVA results and quadratic models of PES-PAC membranes for pure flux and Max. TMP

| Source	Pure flux (L m⁻² h⁻¹)		Max. TMP (bar)	
	F-value	Prob. $> F$	F-value	Prob. $> F$
Model	53.56	<0.0001 (S)[a]	49.62	<0.0001 (S)[a]
A-PES (wt.%)	144.45	<0.0001	131.07	<0.0001
B-PAC (wt.%)	11.86	0.0073	13.01	0.0057
AB	4.38	0.0658	4.78	0.0566
A^2	–	–	–	–
B^2	–	–	–	–
Lack of fit	5.18	0.0681 (NS)[b]	3.38	0.1307 (NS)[b]
	Std. Dev.	7.36	Std. Dev.	0.041
	Mean	70.03	Mean	0.63
	R^2	0.9470	R^2	0.9430
	Adj. R^2	0.9293	Adj. R^2	0.9240
	C.V. %	10.50	C.V. %	6.56
Model equation coded, (wt.%)	$+70.03 - 41.68A + 11.94B - 7.70AB$		$+0.63 + 0.22A - 0.070B - 0.045AB$	

[a]Significant;
[b]Not significant.
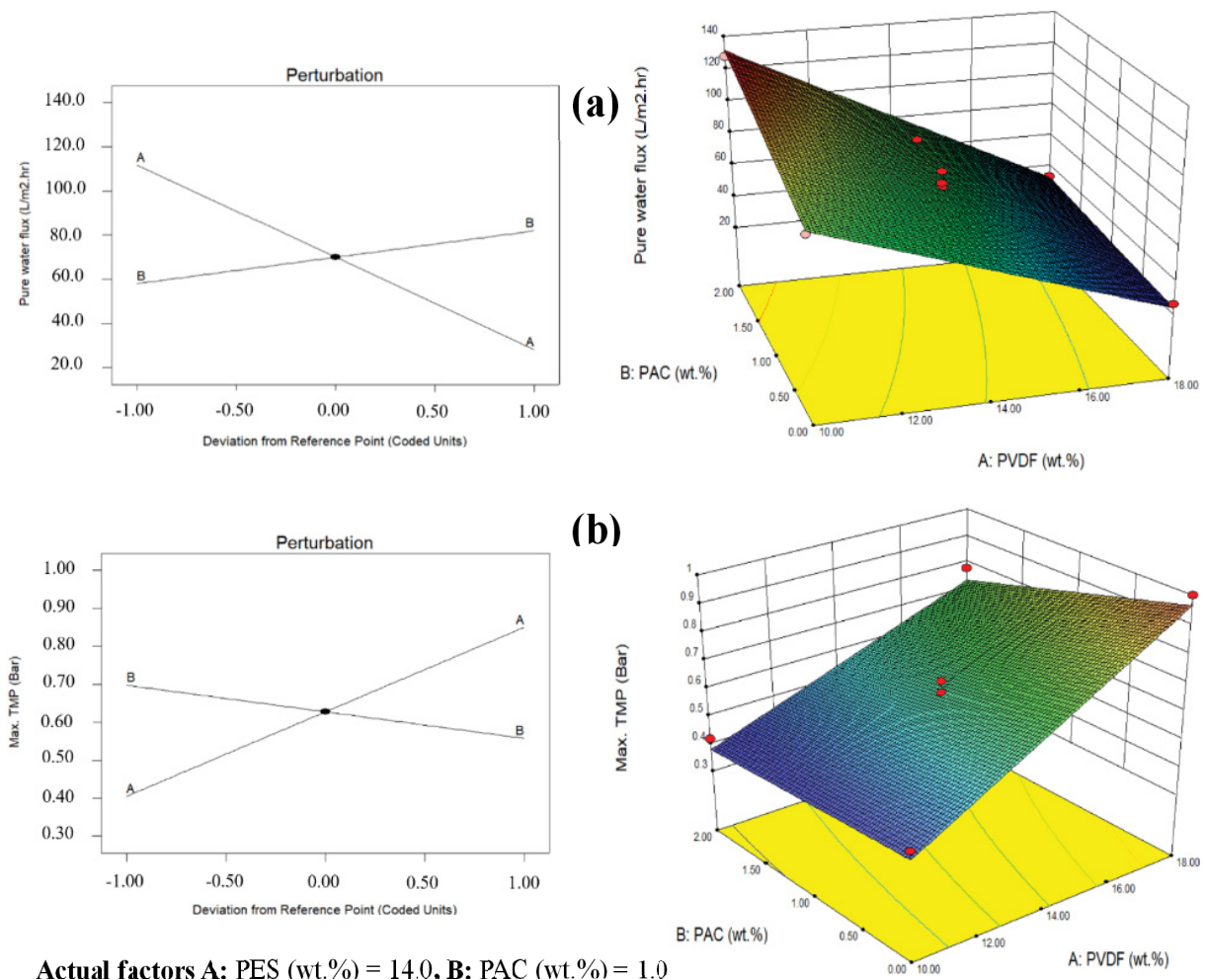
Fig. 7. 3D response surface (right) and perturbation plots (left) of PES-PAC synthesized membrane for (a) pure water flux and (b) Max. TMP.
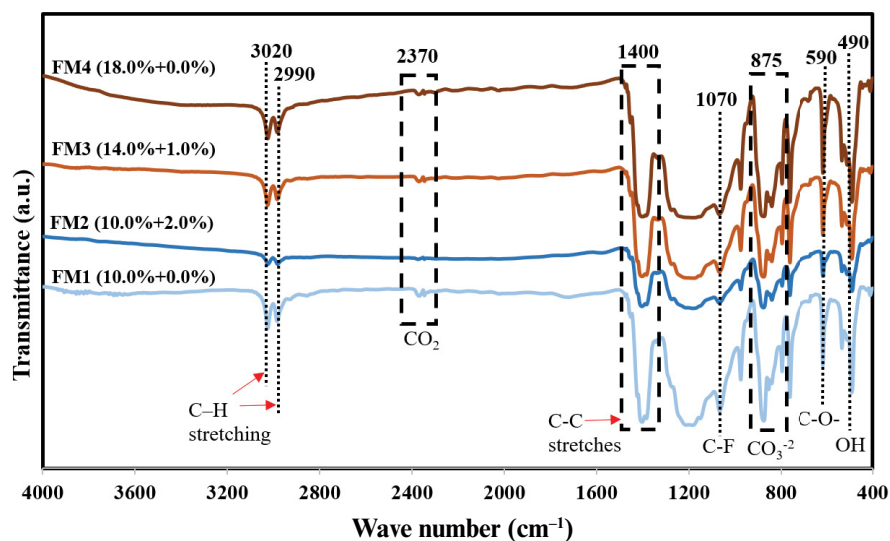
Fig. 8. FTIR spectra for PES-PAC membranes with different concentrations.

others [52], however, in the PES-PAC membranes, the presence of PAC reduced these peaks (FM2 and FM3).

The notable peaks of the various samples around 590, 875 and 2,370 cm^{-1} are assigned to C–O– groups, CO_3^{-2} and CO_2, respectively, were the features distinctive peaks of methanol neutralization applied after membrane casting [53]. Moreover, the OH group detected at 490 cm^{-1} is attributed to the DW that used for membrane solidification during the casting process [54]. Fig. 8 also confirmed that the recorded wavenumbers in spectra of both membranes without PAC (FM1 and FM4) had higher frequencies in comparing with the spectrums of the other two membranes have the PAC content (FM2 and FM3).

Moreover, it could be observed that the peaks of the membrane with greater content of PAC (FM2) had inferior vibrations than that of the other membrane with less content of PAC (FM3). Evidently, the peaks become narrow with less strength at the increasing of PAC weight, indicating that the hydrogen bonds were constructed well between PES polymer chains and the hydroxyl groups from PAC, which reduces the PES hydrophobic tendency [55]. These outcomes confirmed that PAC was well integrated to PES membrane and partially relocated on the membrane surface, which leads to membrane treatment efficiency enhancement.

Furthermore, AFM test was carried out to investigate the membrane top surface along with its roughness as shown in Fig. 9. FM2 membrane might be contain some extra PAC particles which made its top surface rougher compared to others (Fig. 9b). Having less depth of facial peaks and valleys, the FM4 membrane surface (Fig. 9d) is relatively smooth due to contain only PES polymer which received a homogeneous mixing at the preparation phase of dope solution [56]. However, the peaks and valleys of FM1 and FM3 membranes reduced gradually compared to FM2, where FM3 has the smoothest surface compared with other membranes (Fig. 9a–d). To confirm all above observations, the values of membrane surface roughness (R_q and R_a) given in Fig. 9 can be considered.

Fig. 10 presents the FESEM images for produced membranes with different compositions, which show the top surface morphology of membranes along with its cross-section. As can be seen from Fig. 10A–D, there were many small pores available on the surface of FM1 membrane which contains the lowest PES polymer content (10.0 wt.%). On the meantime, the number and size of these pores start to be decreased first on membrane (FM3) with PES content 14.0 wt.% and PAC content 1.0 wt.%, followed by FM2 membrane with the highest PAC content (2.0 wt.%), while the membrane (FM4) has a semi-impermeable surface because of its high PES polymer content (18.0 wt.%) with no PAC content, this was agree with the findings that was early discovered by Kunst and Sourirajan (1974).

As referring to membrane cross-sections on Fig. 10a–d, all membranes display the formation of macrovoid with loosely packed structures. Typically, the membrane consists of two layers, which are a spongy porous support layer and a dense top finger-like layer. The establishment of these configurations can be attributed to the instantaneous demixing of polymer and solvent during the process of phase inversion.

FM1 membrane has only PES with the weight of 10.0 wt.%, displaying a finger-like morphology and a support layer with sponge-like structure containing large unconnected pores delimited by polymer walls (Fig. 10a). The finger-like vacuums turn into flat, bigger and even strained to the bottom-most of the fabricated membranes with the PAC concentration increasing (FM2 and FM3), and the spherical voids of the sponge-like shape linked more tightly among themselves (Fig. 10b and c). However, FM4 membrane contains the highest concentration of PES, gives thin, smaller and not stretched figure-like holes with lest connection to the little sponge-like pores located on the cross-section's bottom, which produces low membrane flux because greater amount of polymer contributed a higher membrane viscosity which lead to decease the membrane porosity and pore size. However, FM1 and FM4 both have
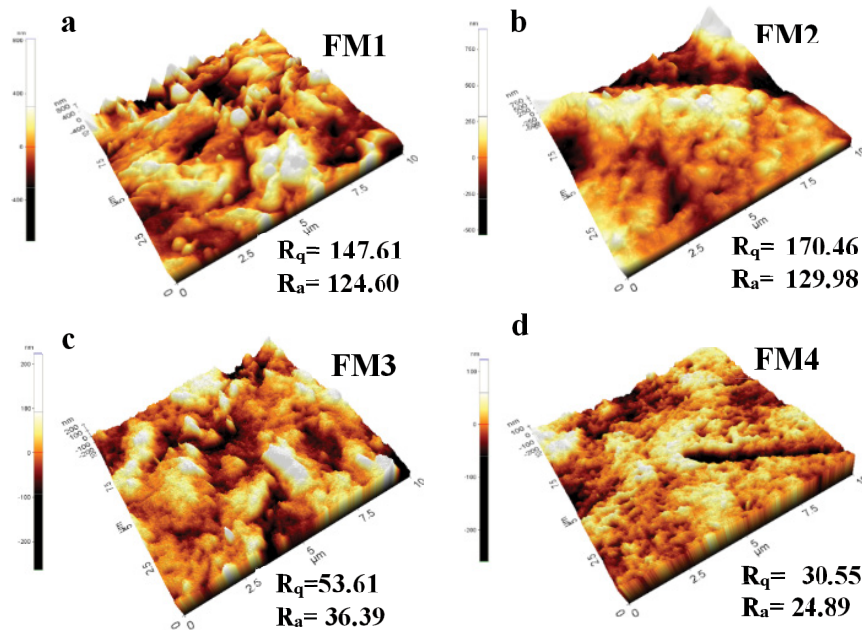
Fig. 9. AFM top surface images with average membrane roughness values (nm) for various compositions of selected PES-PAC membranes: (a–d) for (FM1 to FM4).

no PAC content, they still have different contents of PES polymer, which are 10.0% and 18.0%, respectively. Therefore, the surface structure as well as the cross-section was totally different. The overall FESEM micrographs have proved the significant effect of the PAC presence in improving the fabricated membrane characteristic in term of membrane rejection and therefore removal rate of contaminants.

For membrane permeability analysis, the impact of PAC adding in membrane permeability in terms of porosity and average pore size; as permeability indicators, were evaluated for the produced PES membranes. As presented in Table 5, the porosity and average pore size of the fabricated PES membranes incorporated with PAC were higher compared with other membranes without PAC. Based on Table 5, the resulted fabricated membranes were "microfiltration" and the maximum porosity mean values and average pore size were attained in FM2 membrane at the values 77.48% and 24.43 µm, respectively, however, the lowermost values of the same consistent permeability parameters were found using membrane FM4 at 48.38% and 12.15 µm, respectively. These findings were totally agreed with the above morphological results.

3.7. Membrane treatment optimization

The best synthesized membrane has been selected using RSM tool, where the membrane efficiencies of COD, colour and NH_3–N removal were optimized during this study.

Based on the DoE software, the operational conditions (PES weight, PAC weight) were targeted to be within the range. While the dependents of treatment performance (NH_3–N, colour and COD removal) were chosen as "maximum" to get the ultimate filtration performance. The additional responses were remained "within the range".

Accordingly, the optimization tool assimilates the singular attractiveness into a particular number, and then look for optimizing the function.

Consequently, the composition of the optimum membrane together with respective rates of removal efficiency were obtained. The optimum removals beside the corresponding water flux and Max. TMP are presented in Table 6.

Membrane with 14.9 wt.% of PES and 1.0 wt.% of PAC was found to be the optimum, and thus selected as the best membrane design having optimum removal efficiency according to its highest desirability (0.870) [58].

As shown in Table 6, 22.00%, 48.71% and 35.34% removal of NH_3–N, colour and COD respectively, was forecast by the software using optimized operational conditions. The corresponding (Non-optimized) water flux and Max. TMP were found at the values 61.00 L m^{-2} h^{-1} and 0.67 bar, respectively. An additional experimentation was then performed to confirm the optimum findings.

As illustrated in Table 6, the error column indicates the differences between the predicted and laboratory values, which shows that the lab experiments agree well with the response values estimated by the software. However, less agreement between the predicted and the laboratory result was obtained in case of NH_3–N removal (8.36% error).

4. Conclusions

The adsorbent material PAC was used to fabricate a novel PES membrane using the process of phase inversion. The fabricated PES flat sheet membranes integrated with PAC showed superior efficiencies than that of the pure PES membrane, which effectively developed the removal rate and the fouling control parameters of produced membranes. However, increasing PAC content to a certain value
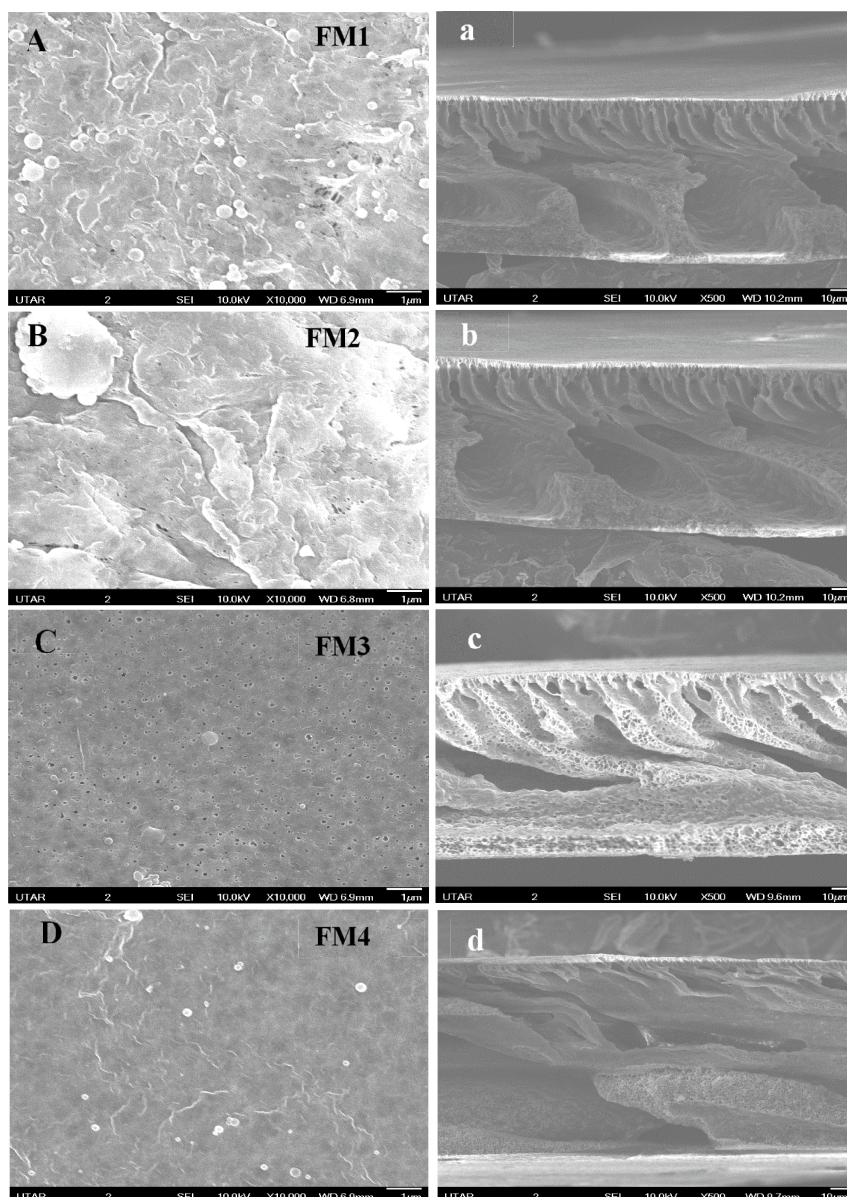
Fig. 10. FESEM images of PES-PAC membranes with numerous compositions (FM1 to FM4): (a–d) cross-sections and (A–D) top surfaces.

Table 5
Porosity and average pore size for selected fabricated PES-PAC membranes

Membrane	Composition		Porosity (%)[a]	Average pore size (μm)[a]
	PES	PAC		
FM1	10.0	0.0	57.25 ± 0.18	15.34 ± 0.05
FM2	10.0	2.0	77.48 ± 0.50	24.43 ± 0.15
FM3	14.0	1.0	72.86 ± 0.20	21.27 ± 0.07
FM4	18.0	0.0	48.38 ± 0.62	12.15 ± 0.24

[a]Each parameter is expressed as average value ± standard deviation.

has a positive influence on the removal efficiency of COD, colour and NH_3–N. Furthermore, FTIR and the morphological investigations have presented the better effect of PAC existence on membrane surface. Operational optimization was done using RSM to select the optimum membrane design in terms of the elimination performances. Best membrane composition was found using (14.9 wt.%) PES and (1.0 wt.%) PAC, which removed 36.63% from COD, 49.50% from colour and 23.84% from NH_3–N content. This was agreed with the predicted removals based on the small calculated error. The corresponding experimental values of water flux and Max. TMP found also agreed with the predicted one with the values of 61.10 L m^{-2} h^{-1} and 0.64 bar, respectively. The performance and structure of fabricated membranes were investigated by filtration tests, FTIR,

Table 6
Predicted and experimental removal efficiencies of the optimum PES-PAC membrane with the corresponding operating condition

Operating conditions		Desirability	Optimum conditions	
PES (wt.%)	PAC (wt.%)			
14.90	1.00	0.870	Selected	
Response		Predicted result	Experimental result	Error (%)
Removal of COD (%)[a]		35.34	36.63	3.65
Removal of colour (%)[a]		48.71	49.50	1.62
Removal of NH_3–N (%)[a]		22.00	23.84	8.36
Pure water flux (L m^{-2} h^{-1})		61.00	61.10	0.16
Max. TMP (bar)		0.67	0.64	4.48

[a]Optimum value.

FESEM, and AFM spectroscopy. Generally, present report shows the treatment and hydrophilic improvement of hydrophobic PES polymer membranes using PAC. For further removal efficiency, membrane properties or practice could be improved by either adding a hydrophilic material, or applying pre-treatment process like adsorption via PAC.

References

[1]   Y. Xu, C. Chen, X. Li, J. Lin, Y. Liao, Z. Jin, Recovery of humic substances from leachate nanofiltration concentrate by a two-stage process of tight ultrafiltration membrane, J. Cleaner Prod., 161 (2017) 84–94.

[2]   M.J.K. Bashir, Y.Z. Jun, L.J. Yi, M.F.M. Abushammala, S.S. Abu Amr, L.M. Pratt, Appraisal of student's awareness and practices on waste management and recycling in the Malaysian University's student hostel area, J. Mater. Cycles Waste Manage., 22 (2020) 916–927.

[3]   S.M.A. Abuabdou, W. Ahmad, N.C. Aun, M.J.K. Bashir, A review of anaerobic membrane bioreactors (AnMBR) for the treatment of highly contaminated landfill leachate and biogas production: Effectiveness, limitations and future perspectives, J. Cleaner Prod., 255 (2020) 120215, doi: 10.1016/j.jclepro.2020.120215.

[4]   N.B. Azmi, M.J.K. Bashir, S. Sethupathi, C.A. Ng, Anaerobic stabilized landfill leachate treatment using chemically activated sugarcane bagasse activated carbon: kinetic and equilibrium study, Desal. Water Treat., 57 (2016) 3916–3927.

[5]   S.M.A. Abuabdou, O.W. Teng, M.J.K. Bashir, N.C. Aun, S. Sethupathi, L.M. Pratt, Treatment of tropical stabilised landfill leachate using palm oil fuel ashisothermal and kinetic studies, Desal. Water Treat., 144 (2019) 201–210.

[6]   T.J.H. Banch, M.M. Hanafiah, A.F.M. Alkarkhi, S.S. Abu Amr, Factorial design and optimization of landfill leachate treatment using tannin-based natural coagulant, Polymers (Basel), 11 (2019) 1–15, doi: 10.3390/polym11081349.

[7]   Q. Xu, G. Siracusa, S. Di Gregorio, Q. Yuan, COD removal from biologically stabilized landfill leachate using advanced oxidation processes (AOPs), Process Saf. Environ. Prot., 120 (2018) 278–285.

[8]   S.Y. Guvenc, K. Dincer, G. Varank, Performance of electrocoagulation and electro-Fenton processes for treatment of nanofiltration concentrate of biologically stabilized landfill leachate, J. Water Process Eng., 31 (2019) 100863, doi: 10.1016/j.jwpe.2019.100863.

[9]   S.S. Abu Amr, S.N.F. Zakaria, H.A. Aziz, Performance of combined ozone and zirconium tetrachloride in stabilized landfill leachate treatment, J. Mater. Cycles Waste Manage., 19 (2016) 1384–1390.

[10] M. Zielińska, D. Kulikowska, M. Stańczak, Adsorption – membrane process for treatment of stabilized municipal landfill leachate, Waste Manage., 114 (2020) 174–182.

[11] S.M.A. Abuabdou, M.J.K. Bashir, N.C. Aun, S. Sethupathi, Applicability of anaerobic membrane bioreactors for landfill leachate treatment: review and opportunity, IOP Conf. Ser.: Earth Environ. Sci., 140 (2018) 012033–012042.

[12] J. Shen, Q. Zhang, Q. Yin, Z. Cui, W. Li, W. Xing, Fabrication and characterization of amphiphilic PVDF copolymer ultrafiltration membrane with high anti-fouling property, J. Membr. Sci., 521 (2017) 95–103.

[13] C.A. Ng, L.Y. Wong, M.J.K. Bashir, S.L. Ng, Development of hybrid polymeric polyerthersulfone (PES) membrane incorporated with powdered activated carbon (PAC) for palm oil mill effluent (POME) treatment, Int. J. Integr. Eng. Spec. Issue Civ. Environ. Eng., 10 (2018) 137–141.

[14] P. Krzeminski, L. Leverette, S. Malamis, E. Katsou, Membrane bioreactors – a review on recent developments in energy reduction, fouling control, novel configurations, LCA and market prospects, J. Membr. Sci., 527 (2017) 207–227.

[15] A. Shehzad, M.J.K. Bashir, S. Sethupathi, J. Lim, Simultaneous removal of organic and inorganic pollutants from landfill leachate using sea mango derived activated carbon via microwave induced activation, Int. J. Chem. Reactor Eng., 14 (2016) 991–1001.

[16] D.J. Miller, D.R. Paul, B.D. Freeman, An improved method for surface modification of porous water purification membranes, Polymer (Guildf), 55 (2014) 1375–1383.

[17] S. Jankhah, P.R. Bérubé, Pulse bubble sparging for fouling control, Sep. Purif. Technol., 134 (2014) 58–65.

[18] B. Venkataganesh, A. Maiti, S. Bhattacharjee, S. De, Electric field assisted cross flow micellar enhanced ultrafiltration for removal of naphthenic acid, Sep. Purif. Technol., 98 (2012) 36–45.

[19] J.C. Crittenden, R.R. Trussell, D.W. Hand, K.J. Howe, G. Tchobanoglous, MWH's Water Treatment: Principles and Design, John Wiley & Sons, New Jersey, USA, 2012.

[20] N.H. Ismail, W.N.W. Salleh, A.F. Ismail, H. Hasbullah, N. Yusof, F. Aziz, J. Jaafar, Hydrophilic polymer-based membrane for oily wastewater treatment: a review, Sep. Purif. Technol., 233 (2020) 116007, doi: 10.1016/j.seppur.2019.116007.

[21] N.I.M. Nawi, M.R. Bilad, N.A.H.M. Nordin, M.O. Mavukkandy, Z.A. Putra, M.D.H. Wirzal, J. Jaafar, A.L. Khan, Exploiting the interplay between liquid-liquid demixing and crystallization of the PVDF membrane for membrane distillation, Int. J. Polym. Sci., 2018 (2018) 1–10, doi: 10.1155/2018/1525014.

[22] J. Ji, F. Liu, N. Awanis Hashim, M.R. Moghareh Abed, K. Li, Poly(vinylidene fluoride) (PVDF) membranes for fluid separation, React. Funct. Polym., 86 (2015) 134–153.

[23] M.J.K. Bashir, T.M. Xian, A. Shehzad, S. Sethupathi, N.C. Aun, S.A. Amr, Sequential treatment for landfill leachate by applying coagulation–adsorption process, Geosyst. Eng., 20 (2017) 9–20.

[24] J. Lv, G. Zhang, H. Zhang, C. Zhao, F. Yang, Improvement of antifouling performances for modified PVDF ultrafiltration membrane with hydrophilic cellulose nanocrystal, Appl. Surf. Sci., 440 (2018) 1091–1100.

[25] N.M. Mokhtar, W.J. Lau, B.C. Ng, A.F. Ismail, D. Veerasamy, Preparation and characterization of PVDF membranes incorporated with different additives for dyeing solution treatment using membrane distillation, Desal. Water Treat., 56 (2015) 1999–2012.

[26] A. Zhou, R. Jia, Y. Wang, S. Sun, X. Xin, M. Wang, Q. Zhao, H. Zhu, Abatement of sulfadiazine in water under a modified ultrafiltration membrane (PVDF-PVP-TiO$_2$-dopamine) filtration-photocatalysis system, Sep. Purif. Technol., 234 (2020) 116099, doi: 10.1016/j.seppur.2019.116099.

[27] J.H. Jhaveri, Z.V.P. Murthy, A comprehensive review on anti-fouling nanocomposite membranes for pressure driven membrane separation processes, Desalination, 379 (2016) 137–154.

[28] J. Zhang, Q. Wang, Z. Wang, C. Zhu, Z. Wu, Modification of poly(vinylidene fluoride)/polyethersulfone blend membrane with polyvinyl alcohol for improving antifouling ability, J. Membr. Sci., 466 (2014) 293–301.

[29] L.Y. Wong, C.A. Ng, M.J.K. Bashir, C.K. Cheah, K. Leong, Membrane bioreactor performance improvement by adding adsorbent and coagulant: a comparative study, Desal. Water Treat., 57 (2015) 13433–13439.

[30] S. Wong, N. Ngadi, I.M. Inuwa, O. Hassan, Recent advances in applications of activated carbon from biowaste for wastewater treatment: a short review, J. Cleaner Prod., 175 (2018) 361–375.

[31] M.J.K. Bashir, J.W. Wong, S. Sethupathi, N.C. Aun, L.J. Wei, Preparation of palm oil mill effluent sludge biochar for the treatment of landfill leachate, MATEC Web Conf., 103 (2017) 1–8, doi: 10.1051/matecconf/201710306008.

[32] APHA, Water Environment Federation, Standard Methods for the Examination of Water and Wastewater, 22nd ed., Washington, DC, 2012.

[33] S.M.A. Abuabdou, M.J.K. Bashir, N.C. Aun, S. Sethupathi, W.L. Yong, Development of a novel polyvinylidene fluoride membrane integrated with palm oil fuel ash for stabilized landfill leachate treatment, J. Cleaner Prod., 311 (2021) 127677, doi: 10.1016/j.jclepro.2021.127677.

[34] M. Mertens, T. Van Dyck, C. Van Goethem, A.Y. Gebreyohannes, I.F.J. Vankelecom, Development of a polyvinylidene di fluoride membrane for nano filtration, J. Membr. Sci., 557 (2018) 24–29.

[35] S.T. Tan, W.S. Ho, H. Hashim, C.T. Lee, M.R. Taib, C.S. Ho, Energy, economic and environmental (3E) analysis of waste-to-energy (WTE) strategies for municipal solid waste (MSW) management in Malaysia, Energy Convers. Manage., 102 (2015) 111–120.

[36] S.S. Abu Amr, H.A. Aziz, M.J.K. Bashir, Application of response surface methodology (RSM) for optimization of semi-aerobic landfill leachate treatment using ozone, Appl Water Sci., 4 (2014) 231–239.

[37] Stat-Ease Inc., Multifactor RSM Tutorial, 2016.

[38] S. Naragintia, Y.-Y. Yua, Z. Fanga, Y.-C. Yong, Novel tetrahedral Ag$_3$PO$_4$@N-rGO for photocatalytic detoxification of sulfamethoxazole: process optimization, transformation pathways and biotoxicity assessment, Chem. Eng. J., 375 (2019) 122035, doi: 10.1016/j.cej.2019.122035.

[39] Z.A. Ghani, M. Suffian, N. Qamaruz, M. Faiz, M. Ahmad, Optimization of preparation conditions for activated carbon from banana pseudo-stem using response surface methodology on removal of color and COD from landfill leachate, Waste Manage., 62 (2017) 177–187.

[40] I.A. Ike, L.F. Dumée, A. Groth, J.D. Orbell, M. Duke, Effects of dope sonication and hydrophilic polymer addition on the properties of low pressure PVDF mixed matrix membranes, J. Membr. Sci., 540 (2017) 200–211.

[41] S. Nejati, C. Boo, C.O. Osuji, M. Elimelech, Engineering flat sheet microporous PVDF films for membrane distillation, J. Membr. Sci., 492 (2015) 355–363.

[42] H. Fan, Y. Peng, Application of PVDF membranes in desalination and comparison of the VMD and DCMD processes, Chem. Eng. Sci., 79 (2012) 94–102.

[43] H.A. Aziz, A. Mojiri, Wastewater Engineering: Advanced Wastewater Treatment Systems, 1st ed., IJSR Publications, Penang, Malaysia, 2014. Available at: https://doi.org/10.12983/1-2014-03-01

[44] T. Chidambaram, Y. Oren, M. Noel, Fouling of nanofiltration membranes by dyes during brine recovery from textile dye bath wastewater, Chem. Eng. J., 262 (2015) 156–168.

[45] Y. Zheng, W. Zhang, B. Tang, J. Ding, Y. Zheng, Z. Zhang, Membrane fouling mechanism of biofilm-membrane bioreactor (BF-MBR): pore blocking model and membrane cleaning, Bioresour. Technol., 250 (2018) 398–405.

[46] X. Chen, B. Zhao, L. Zhao, S. Bi, P. Han, X. Feng, L. Chen, Temperature- and pH-responsive properties of poly(vinylidene fluoride) membranes functionalized by blending microgels, RSC Adv., 4 (2014) 29933–29945.

[47] Department of Environment, Ministry of Natural Resources and Environment, Environmental requirements: A Guide for Investors, 11th ed., Malaysia, 2010.

[48] A. Kemal, K. Siraj, W.H. Michael, Adsorption of Cu(II) and Cd(II) onto activated carbon prepared from pumpkin seed shell, J. Environ. Sci. Pollut. Res., 5 (2019) 328–333.

[49] M. Aslam, R. Ahmad, J. Kim, Recent developments in biofouling control in membrane bioreactors for domestic wastewater treatment, Sep. Purif. Technol., 206 (2018) 297–315.

[50] I. Ali, O.A. Bamaga, L. Gzara, M. Bassyouni, M.H. Abdel-Aziz, M.F. Soliman, E. Drioli, M. Albeirutty, Assessment of blend PVDF membranes, and the effect of polymer concentration and blend composition, Membranes, 8 (2018) 1–19, doi: 10.3390/membranes8010013.

[51] E. Fumoto, S. Sato, T. Takanohashi, Determination of carbonyl functional groups in heavy oil using infrared spectroscopy, Energy Fuels, 34 (2020) 5231–5235.

[52] S.M.A. Abuabdou, Z.H. Jaffari, C.A. Ng, Y.C. Ho, M.J.K. Bashir, A new polyvinylidene fluoride membrane synthesized by integrating of powdered activated carbon for treatment of stabilized leachate, Water (Switzerland), 13 (2021), doi: 10.3390/w13162282.

[53] B.E. Gurkan, J.C. de la Fuente, E.M. Mindrup, L.E. Ficke, B.F. Goodrich, E.A. Price, W.F. Schneider, A.J.F. Brennecke, Equimolar CO$_2$ absorption by anion-functionalized ionic liquids, J. Am. Chem. Soc., 132 (2010) 2116–2117.

[54] D. Guo, Y. Xiao, T. Li, Q. Zhou, L. Shen, R. Li, Y. Xu, H. Lin, Fabrication of high-performance composite nanofiltration membranes for dye wastewater treatment: mussel-inspired layer-by-layer self-assembly, J. Colloid Interface Sci., 560 (2020) 273–283.

[55] J. Zhang, Z. Wang, Q. Wang, J. Ma, J. Cao, W. Hu, Z. Wu, Relationship between polymers compatibility and casting solution stability in fabricating PVDF/PVA membranes, J. Membr. Sci., 537 (2017) 263–271.

[56] J. Tae, J.F. Kim, H.H. Wang, E. di Nicolo, E. Drioli, Y.M. Lee, Understanding the non-solvent induced phase separation (NIPS) effect during the fabrication of microporous PVDF membranes *via* thermally induced phase separation (TIPS), J. Membr. Sci., 514 (2016) 250–263.

[57] B. Kunst, S. Sourirajan, An approach to the development of cellulose acetate ultrafiltration membranes, J. Appl. Polym. Sci., 18 (1974) 3423–3434.

[58] M.A. Bezerra, R.E. Santelli, E.P. Oliveira, L.S. Villar, L.A. Escaleira, Response surface methodology (RSM) as a tool for optimization in analytical chemistry, Talanta, 76 (2008) 965–977.